

Andreev bound states and tunneling characteristics of a non-centrosymmetric superconductor

C. Iniotakis,¹ N. Hayashi,¹ Y. Sawa,² T. Yokoyama,² U. May,¹ Y. Tanaka,² and M. Sigrist^{1,3}

¹*Institute for Theoretical Physics, ETH Zurich, 8093 Zurich, Switzerland*

²*Department of Applied Physics, Nagoya University, Nagoya, 464-8603, Japan*

³*Department of Physics, Kyoto University, Kyoto 606-8502, Japan*

(Dated: September 29, 2018)

The tunneling characteristics of planar junctions between a normal metal and a non-centrosymmetric superconductor like CePt₃Si are examined. It is shown that the superconducting phase with mixed parity can give rise to characteristic zero-bias anomalies in certain junction directions. The origin of these zero-bias anomalies are Andreev bound states at the interface. The tunneling characteristics for different directions allow to test the structure of the parity-mixed pairing state.

PACS numbers: 74.20.Rp, 74.70.Tx, 74.45.+c

Since the early sixties tunneling spectroscopy has played an important role in gathering information about the gap function of conventional superconductors [1]. In the context of unconventional superconductivity tunneling appeared as a tool to probe the internal phase structure of the Cooper pair wave functions. Surface states with sub-gap energy, known as Andreev bound states, provide channels for resonant tunneling leading to so-called zero-bias anomalies. Zero-bias anomalies observed in high-temperature superconductors showed the presence of zero-energy bound states at the surface, giving strong evidence for *d*-wave pairing [2, 3, 4, 5, 6]. Similarly the tunneling spectrum observed in Sr₂RuO₄ is consistent with the existence of chiral surface states as expected for a chiral *p*-wave superconductor [7, 8, 9, 10, 11]. Thus quasiparticle tunneling has emerged as an important phase sensitive probe for unconventional superconductors.

The recent discovery of superconductivity in the heavy Fermion compound CePt₃Si has motivated intense experimental and theoretical studies, since its crystal symmetry is lacking a center of inversion [12, 13, 14, 15, 16]. It was shown that the presence of antisymmetric spin-orbit coupling in such a material could be responsible for a number of intriguing phenomena, such as the rather high upper critical field exceeding the standard paramagnetic limit [12, 13]. The absence of inversion symmetry yields a classification scheme of the pairing symmetry, different from the standard distinction between even- and odd-parity states. Actually, the pairing states in these non-centrosymmetric superconductors can be viewed as states of mixed parity which do not have a definite spin-singlet or spin-triplet configuration, either. For CePt₃Si various experiments can be interpreted in a way that the pairing state has the highest possible symmetry, but would develop line nodes in the gap due to a mixing of the *s*-wave and a *p*-wave component. This state belongs to the *A*₁-representation of the generating tetragonal point group *C*_{4v} for CePt₃Si. While thermodynamic quantities give good evidence for this behavior, it would be desirable

to have additional proof for this kind of state through a phase sensitive test. The characteristics of quasiparticle tunneling may provide such a means. Despite the fact that the parity mixing *A*₁-phase has the full symmetry of the system, it gives rise to characteristic non-trivial features in the tunneling spectra (cf. also [17]).

In the present study, we address the problem of possible Andreev bound states at the boundaries of a non-centrosymmetric superconductor like CePt₃Si and demonstrate that quasiparticle tunneling could give important information on the gap structure of such a material. The theoretical framework for our calculations is given by the quasiclassical Eilenberger theory [18, 19, 20]. Our starting point is the quasiclassical bulk propagator \check{g}_B in a non-centrosymmetric superconductor with antisymmetric Rashba-type spin-orbit coupling, which has already been derived in Ref. [16]:

$$\check{g}_B = -i\pi \begin{pmatrix} \hat{g} & i\hat{f} \\ -i\hat{f} & -\hat{g} \end{pmatrix}, \quad (1)$$

where the upper two components are given as

$$\hat{g} = \frac{\omega_n}{\sqrt{\omega_n^2 + |\Delta_+|^2}} \hat{\sigma}_+ + \frac{\omega_n}{\sqrt{\omega_n^2 + |\Delta_-|^2}} \hat{\sigma}_- \quad (2)$$

$$\hat{f} = \left(\frac{\Delta_+}{\sqrt{\omega_n^2 + |\Delta_+|^2}} \hat{\sigma}_+ + \frac{\Delta_-}{\sqrt{\omega_n^2 + |\Delta_-|^2}} \hat{\sigma}_- \right) i\hat{\sigma}_y \quad (3)$$

and similar relations hold for the lower components \hat{f} and \hat{g} . On the right hand side of Eqs. (2) and (3), $\omega_n = (2n+1)\pi k_B T$ denotes the Matsubara frequency, and both the gap amplitudes Δ_{\pm} and the spin matrices $\hat{\sigma}_{\pm}$ are $\hat{\mathbf{k}}$ -dependent. For a spherical Fermi surface parametrized in the standard way by $\hat{\mathbf{k}} = (\cos \phi \sin \theta, \sin \phi \sin \theta, \cos \theta)$, the gap amplitudes are

$$\Delta_{\pm} = \psi \pm \Delta \sin \theta, \quad (4)$$

while the spin matrices may be written as

$$\hat{\sigma}_{\pm} = \frac{1}{2} \begin{pmatrix} 1 & \mp i e^{-i\phi} \\ \pm i e^{i\phi} & 1 \end{pmatrix}. \quad (5)$$

The variables ψ and Δ are taken to be real and denote the gap amplitudes of the s - and p -wave components of the parity-mixed superconducting state. Altogether, this result is interpreted as a superconducting phase on two split spherical Fermi surfaces, each of them having a non-trivial gap function with amplitudes given by Eq. (4) and complex spin structures according to Eq. (5). For technical simplicity we assume here that the splitting is small, such that both Fermi surfaces have identical size and a description by a one-band formalism is possible as described by Eqs. (1)-(5). A generalization to a really split Fermi surface is straightforward, but requires a more extended notation without giving additional insights.

In order to finally include the boundary effects, it is convenient to use the Riccati-parametrization of the quasiclassical theory [21, 22]. Within this technique, the full quasiclassical propagator \check{g} in combined particle-hole and spin space may be written in terms of two coherence functions γ and $\tilde{\gamma}$ in the following way [22]:

$$\check{g} = -i\pi \begin{pmatrix} (1 - \gamma\tilde{\gamma})^{-1} & 0 \\ 0 & (1 - \tilde{\gamma}\gamma)^{-1} \end{pmatrix} \begin{pmatrix} 1 + \gamma\tilde{\gamma} & 2\gamma \\ -2\tilde{\gamma} & -1 - \tilde{\gamma}\gamma \end{pmatrix} \quad (6)$$

The coherence functions $\gamma, \tilde{\gamma}$ themselves are 2×2 -spin matrices, which contain local information about the particle-hole coherence for a given $\hat{\mathbf{k}}$ -direction. Particularly, γ_B and $\tilde{\gamma}_B$ in the bulk of a non-centrosymmetric superconductor can be obtained just by comparing the known result of Eqs. (1)-(3) with the general form in Eq. (6), leading to:

$$\gamma_B = i(1 + \hat{g})^{-1} \hat{f} \quad (7a)$$

$$\tilde{\gamma}_B = i\hat{f}^{-1}(1 - \hat{g}), \quad (7b)$$

which can be written as

$$\gamma_B = -(\gamma_+ \hat{\sigma}_+ + \gamma_- \hat{\sigma}_-) \hat{\sigma}_y \quad (8a)$$

$$\tilde{\gamma}_B = \hat{\sigma}_y (\gamma_+ \hat{\sigma}_+ + \gamma_- \hat{\sigma}_-), \quad (8b)$$

where we define

$$\gamma_{\pm} = \frac{\Delta_{\pm}}{\omega_n + \sqrt{\omega_n^2 + |\Delta_{\pm}|^2}}. \quad (9)$$

The advantage of this Riccati formalism is, that spatial inhomogeneities such as the boundaries can be taken into account in a straightforward way [22, 23, 24].

In the vicinity of the boundary the pair potential can develop a spatial dependence and deviate from the bulk form. Since we focus mainly on the qualitative aspects, however, we ignore this effect in the following and assume the gap is constant throughout the superconductor. The usual procedure within the Riccati formalism, namely solving differential equations of the Riccati type numerically for given $\hat{\mathbf{k}}$ -direction, is unnecessary in this case. The presence of the surface enters through rather simple boundary conditions for the coherence functions [22].

For an impenetrable interface, the coherence functions $\gamma_S, \tilde{\gamma}_S$ at the surface of the superconductor are given analytically in terms of the bulk coherence functions:

$$\gamma_S(\hat{\mathbf{k}}_{\text{out}}) = \gamma_B(\hat{\mathbf{k}}_{\text{in}}) \quad \tilde{\gamma}_S(\hat{\mathbf{k}}_{\text{out}}) = \tilde{\gamma}_B(\hat{\mathbf{k}}_{\text{out}}). \quad (10)$$

Here $\hat{\mathbf{k}}_{\text{in}}$ and $\hat{\mathbf{k}}_{\text{out}}$ denote the incoming and outgoing directions of the wave vector, which are connected through the condition of specular scattering. Now the full quasiclassical propagator \check{g}_S at the boundary is easily generated from the coherence functions according to Eq. (10). From $\check{g}_{S,11}$ we obtain, for example, the angular resolved local density of states at the boundary of the non-centrosymmetric superconductor:

$$N(E, \hat{\mathbf{k}}) \quad (11) \\ = N_0 \frac{1}{2} \text{Re} \left[\text{tr} \left((1 - \gamma_S \tilde{\gamma}_S)^{-1} (1 + \gamma_S \tilde{\gamma}_S) \right) \Big|_{i\omega_n \rightarrow E + i0^+} \right],$$

where E denotes the quasiparticle energy and N_0 is the density of states of the normal state. With $\langle \dots \rangle$ denoting an average over the Fermi surface, the local density of states is just given as $N(E) = \langle N(E, \hat{\mathbf{k}}) \rangle$. Note, that at the boundary it is sufficient to average over half of the Fermi sphere only, i.e. we can restrict ourselves to quasiparticles traveling in $\hat{\mathbf{k}}_{\text{out}}$ directions.

Eventually, we also obtain the normalized differential tunneling conductance for a normal metal/non-centrosymmetric superconductor junction at low temperatures $T \ll T_c$. To first order of the interface transmission probability, it can be generated from the angular resolved local density of states of Eq. (11) in the following way [25]:

$$G(eV) = \langle \cos \alpha D(\alpha) N(eV, \hat{\mathbf{k}}) \rangle \langle \cos \alpha D(\alpha) \rangle^{-1}. \quad (12)$$

The function $D(\alpha)$ denotes the transmission coefficient of the interface depending on the angle of incidence α , which is related to the normal vector \mathbf{n} of the boundary by $\cos \alpha = \mathbf{n} \cdot \hat{\mathbf{k}}_{\text{out}}$. In accordance with the result for an interface of the δ -function type [2], the transmission coefficient is taken to be

$$D(\alpha) = \frac{D_0 \cos^2 \alpha}{1 - D_0 \sin^2 \alpha}, \quad (13)$$

where the parameter D_0 specifies the maximum transmission coefficient for the angle of normal incidence $\alpha = 0$.

For the surface with normal vector $\mathbf{n} \parallel \mathbf{z}$ the relation between $\hat{\mathbf{k}}_{\text{in}}$ and $\hat{\mathbf{k}}_{\text{out}}$ needed to evaluate $\gamma_B(\hat{\mathbf{k}}_{\text{in}})$ in Eq. (10) is given by $\phi_{\text{in}} = \phi_{\text{out}}$ and $\theta_{\text{in}} = \pi - \theta_{\text{out}}$, and the angle of incidence is $\alpha = \theta_{\text{out}}$. In this situation, we find immediately that $\Delta_{\pm}(\hat{\mathbf{k}}_{\text{in}}) = \Delta_{\pm}(\hat{\mathbf{k}}_{\text{out}})$ and $\sigma_{\pm}(\hat{\mathbf{k}}_{\text{in}}) = \sigma_{\pm}(\hat{\mathbf{k}}_{\text{out}})$, which directly yields $\gamma_S(\hat{\mathbf{k}}_{\text{out}}) = \gamma_B(\hat{\mathbf{k}}_{\text{out}})$. Hence, both γ_S and $\tilde{\gamma}_S$ are finally given by the bulk coherence functions for the *same* $\hat{\mathbf{k}}$ -direction, and therefore the resulting angular resolved density of states $N(E, \hat{\mathbf{k}})$ is identical to the one of the bulk. No

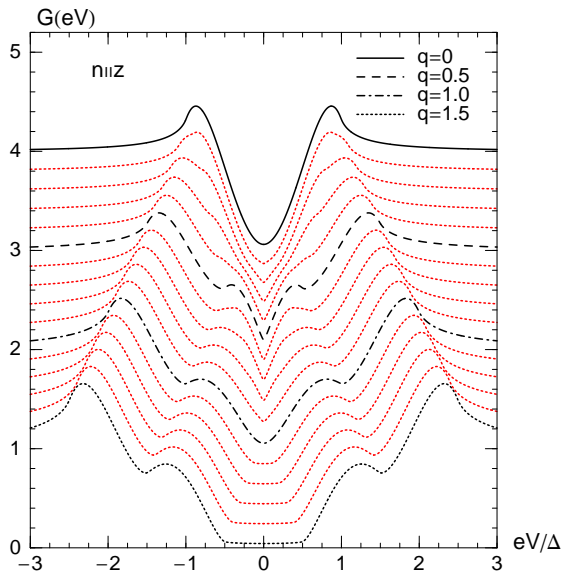


FIG. 1: Normalized low temperature conductance $G(eV)$ for a normal metal/non-centrosymmetric superconductor junction with boundary orientation $\mathbf{n} \parallel \mathbf{z}$. The ratio q of the gap amplitudes is varied from 0 to 1.5 in steps of 0.1. Between two subsequent curves, a vertical offset of 0.2 has been used for clarity of the plot. The transparency of the interface is set to $D_0 = 0.1$.

sub-gap Andreev bound states are generated by surface scattering. For small but finite energies the shape of the local density of states is, however, determined by the actual nodal topology of the gap functions given in Eq. (4). This behavior is then passed on to the resulting tunneling conductances, which are presented in Fig. 1 for different values of the ratio $q = \psi/\Delta$. Starting with $q = 0$, we have a pure p -wave state with point nodes on the poles of the Fermi surface. This leads to a parabolic behavior for low bias voltage reflecting the E^2 -dependence of the density of states. When q is increased, the gap function Δ_+ of Eq. (4) becomes fully gapped (albeit anisotropically), while Δ_- exhibits immediately line nodes developing around the top and bottom of the Fermi sphere. Accordingly, a linear dependence can be observed for low bias. For $q = 1$ the line node of Δ_- has moved to the equator of the Fermi sphere. This removes the linear low-bias behavior in G , since the nodal quasiparticles traveling parallel to the surface cannot contribute to the conductance Eq. (12) any longer. As soon as $q > 1$ however, also the gap function Δ_- is nodeless, which results in the opening of a corresponding gap in the conductance situated between the normalized energies $E/\Delta = \pm|q - 1|$.

Next we turn to the boundary with normal vector $\mathbf{n} \perp \mathbf{z}$ where we can choose freely $\mathbf{n} \parallel \mathbf{y}$. Here, the relation between incoming and outgoing quasiparticle directions is determined by $\phi_{\text{in}} = -\phi_{\text{out}}$ and $\theta_{\text{in}} = \theta_{\text{out}}$. Furthermore, the angle of incidence is $\alpha = \arccos(\sin \phi_{\text{out}} \sin \theta_{\text{out}})$. In

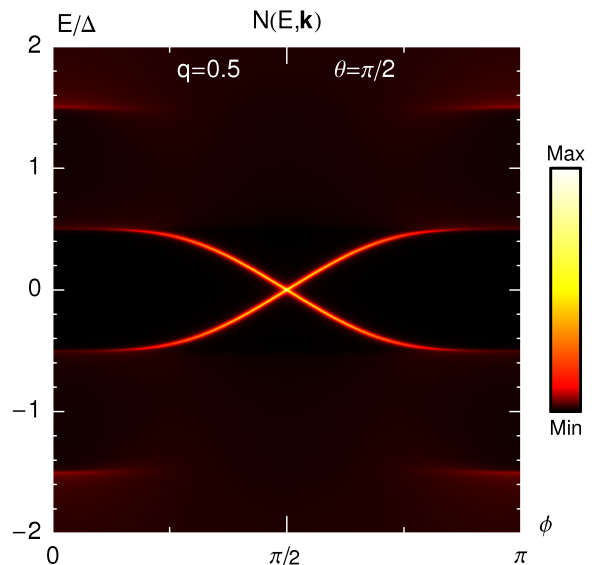


FIG. 2: (color online) Typical angular resolved density of states $N(E, \hat{\mathbf{k}})$ at the boundary of a non-centrosymmetric superconductor with normal vector $\mathbf{n} \parallel \mathbf{y}$. For this example, we set $q = 0.5$ and $\theta = \pi/2$, i.e. we deal with $\hat{\mathbf{k}}$ -vectors of the x, y -plane only. Bright colors represent high spectral weight. The branches of low-energy Andreev bound states according to Eq. (14) are clearly visible.

contrast to $\mathbf{n} \parallel \mathbf{z}$, low-energy Andreev bound states can exist for this orientation. By examination of the angular resolved local density of states $N(E, \hat{\mathbf{k}})$ given in Eq. (11) we find the condition that these bound states only occur for $\hat{\mathbf{k}}$ -vectors with $\Delta_- < 0$, i.e. the contributions come from those parts of the Fermi surface, where the p -wave is stronger than the s -wave ($\sin \theta > q$). Actually, for every angle θ with $\Delta_- < 0$ there is a whole branch of bound states living between the energies $\pm|\Delta_-|$ determined by

$$\cos \phi = \pm \frac{E^2 - \Delta_+ \Delta_- - \sqrt{\Delta_+^2 - E^2} \sqrt{\Delta_-^2 - E^2}}{E(\Delta_+ - \Delta_-)}. \quad (14)$$

Zero-energy Andreev bound states occur for quasiparticle directions with $\phi = \pi/2$ which corresponds to vanishing transverse momentum along the x -direction. An example of the low-energy Andreev bound states in the plane $\theta = \pi/2$ for $q = 0.5$ is provided by Fig. 2.

The normalized low-temperature conductance for this situation is presented in Fig. 3. We find an extended zero-bias conductance peak for $q = 0$, analogous to the one for a pure p -wave superconductor with a cylindrical Fermi surface [7, 8]. This peaked structure at low bias voltages persists as long as $q < 1$ but becomes progressively narrower for $q \rightarrow 1$. These structures are easily understood in the context of the Andreev bound states. For a given $q < 1$ there is always a region around the equator of the Fermi sphere with $\sin \theta > q$, where $\Delta_- < 0$. Quasiparticles from those parts of the Fermi surface support

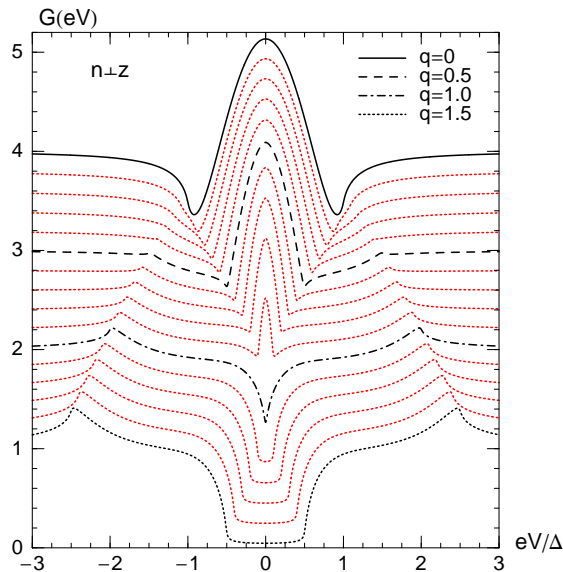


FIG. 3: Normalized low temperature conductance $G(eV)$ for a normal metal/non-centrosymmetric superconductor junction with boundary orientation $\mathbf{n} \perp \mathbf{z}$. The ratio q of the gap amplitudes is varied from 0 to 1.5 in steps of 0.1. Between two subsequent curves, a vertical offset of 0.2 has been used for clarity of the plot. The transparency of the interface is set to $D_0 = 0.1$.

low-energy Andreev bound states up to normalized energies of $\pm|\sin\theta - q|$ according to Eq. (14). The maximum possible energy $\pm|1 - q|$ originates from trajectories at the equator and corresponds to the width of the zero-bias anomalies shown in Fig. 3. Moreover, the total weight around zero bias naturally decreases when q is increased, because the region on the Fermi sphere with $\Delta_- < 0$ is reduced and accordingly the contributions to Andreev bound states. If $q \geq 1$, however, $\Delta_- \geq 0$ everywhere on the Fermi surface and Andreev bound states do not exist anymore. Therefore, the zero-bias anomaly disappears in the tunneling conductance.

The results presented above have been achieved for a typical tunnel junction with small interface transparency $D_0 = 0.1$. Tunnel junctions with other interface transparencies chosen not too large to be consistent with the validity of Eq. (12) show the same characteristic behavior: For boundary orientations $\mathbf{n} \perp \mathbf{z}$ and $q < 1$ the tunneling conductances exhibit a strong zero-bias anomaly.

Our discussion shows that the tunneling characteristics could give important information on the gap structure of non-centrosymmetric superconductors, in particular in view of the parity-mixing. Important is also the direction dependence which would provide an important test for the theoretical picture developed for CePt_3Si so far. It

has also been anticipated that the ratio q could be temperature dependent. Thus it is possible that the tunneling spectrum displays qualitative changes as a function of temperature.

We would like to thank D.F. Agterberg, P.A. Frigeri, K. Wakabayashi and Y. Yanase for helpful discussions. This work was financially supported by the Swiss Nationalfond and the NCCR MaNEP.

-
- [1] I. Giaever, Phys. Rev. Lett. **5**, 147 (1960).
 - [2] C. Bruder, Phys. Rev. B **41**, 4017 (1990).
 - [3] C.R. Hu, Phys. Rev. Lett. **72**, 1526 (1994).
 - [4] Y. Tanaka and S. Kashiwaya, Phys. Rev. Lett. **74**, 3451 (1995).
 - [5] L.J. Buchholtz, M. Palumbo, D. Rainer, and J.A. Sauls, J. Low Temp. Phys. **101**, 1099 (1995).
 - [6] S. Kashiwaya and Y. Tanaka, Rep. Prog. Phys. **63**, 1641 (2000).
 - [7] M. Yamashiro, Y. Tanaka, and S. Kashiwaya, Phys. Rev. B **56**, 7847 (1997).
 - [8] C. Honerkamp and M. Sigrist, J. Low Temp. Phys. **111**, 895 (1998).
 - [9] M. Matsumoto and M. Sigrist, J. Phys. Soc. Jpn. **68**, 994 (1999).
 - [10] F. Laube, G. Goll, H. v. Löhneysen, M. Fogelström, and F. Lichtenberg, Phys. Rev. Lett. **84**, 1595 (2000).
 - [11] Z.Q. Mao, K.D. Nelson, R. Jin, Y. Liu, and Y. Maeno, Phys. Rev. Lett. **87**, 037003 (2001).
 - [12] E. Bauer, G. Hilscher, H. Michor, Ch. Paul, E.W. Scheidt, A. Griбанov, Yu. Seropegin, H. Noël, M. Sigrist, and P. Rogl, Phys. Rev. Lett. **92**, 027003 (2004).
 - [13] P.A. Frigeri, D.F. Agterberg, A. Koga, and M. Sigrist, Phys. Rev. Lett. **92**, 097001 (2004).
 - [14] K.V. Samokhin, E.S. Zijlstra, and S.K. Bose, Phys. Rev. B **69**, 094514 (2004).
 - [15] E. Bauer, I. Bonalde, and M. Sigrist, Low Temp. Phys. **31**, 748 (2005).
 - [16] N. Hayashi, K. Wakabayashi, P.A. Frigeri, and M. Sigrist, Phys. Rev. B **73**, 024504 (2006).
 - [17] T. Yokoyama, Y. Tanaka, and J. Inoue, Phys. Rev. B **72**, 220504(R) (2005).
 - [18] G. Eilenberger, Z. Phys. **214**, 195 (1968).
 - [19] A.I. Larkin and Yu.N. Ovchinnikov, Zh. Éksp. Teor. Fiz. **55**, 2262 (1968); Sov. Phys. JETP **28**, 1200 (1969).
 - [20] J.W. Serene and D. Rainer, Phys. Rep. **101**, 221 (1983).
 - [21] N. Schopohl and K. Maki, Phys. Rev. B **52**, 490 (1995); N. Schopohl, cond-mat/9804064 (1998).
 - [22] M. Eschrig, Phys. Rev. B **61**, 9061 (2000).
 - [23] A.V. Zaitsev, Zh. Éksp. Teor. Fiz. **86**, 1742 (1984); Sov. Phys. JETP **59**, 1015 (1984).
 - [24] A. Shelankov and M. Ozana, Phys. Rev. B **61**, 7077 (2000).
 - [25] Yu.S. Barash and A.A. Svidzinskii, Zh. Éksp. Teor. Fiz. **111**, 1120 (1997); Sov. Phys. JETP **84**, 619 (1997).